The Canadian Mineralogist
Vol. 37, pp. 381-402 (1999)

SUBTLE OSCILLATORY ZONING IN GARNET FROM REGIONAL METAMORPHIC PHYLLITES AND MICA SCHISTS, WESTERN ERZGEBIRGE, GERMANY

RENATE SCHUMACHER[1]

Mineralogisch-Petrologisches Institut, Poppelsdorfer Schloß, Rheinische Friedrich-Wilhelms-Universität, D-53115 Bonn, Germany

KERSTIN RÖTZLER

GeoForschungsZentrum, Telegrafenberg, D-14473 Potsdam, Germany

WALTER V. MARESCH

Institut für Mineralogie, Ruhr-Universität, D-44780 Bochum, Germany

Abstract

Growth zoning patterns of garnet grains in phyllite and mica schist from the Garnet–Phyllite Unit and the Mica–Schist/Eclogite Unit of the Western Erzgebirge, in Saxony, Germany, have been studied in detail by electron microprobe and are characterized with X-ray-intensity mapping images (MAPS) and quantitative chemical analyses. Zoned grains of garnet in the phyllite show a continuous decrease in spessartine component from core (28 mole %) to rim (19 mole %), and, over about 100 μm at the rim, a discontinuous, oscillatory increase, decrease and further increase to 30 mole %. These changes are correlated with an antithetic, oscillatory zoning of comparable amplitude in the almandine component (47% in the core, 56% toward the rim, 49% at the extreme rim). Available data for diffusion rates in garnet suggest that no significant modification of growth zoning attributable to later intracrystalline diffusion has occurred. In two samples of mica schist, oscillatory zoning with respect to the grossular component is correlated with an antithetic pattern of the almandine component (*e.g.*, sample E 514: 17.0 mole % grossular component in the core, decreasing to 4.7 mole %, then increasing to 6.8 mole % and decreasing again to 4.3 mole % at the extreme rim). Although the patterns of zoning in themselves do not yield any evidence of modification after growth, available data on diffusion do not entirely rule out this possibility. In agreement with the observed textural relationships, we attribute the oscillatory changes in garnet composition to specific continuous reactions during regional metamorphism, indicating a complex growth-and-resorption history of the garnet resulting from small-scale variations in the rate of decompression of the rocks. No evidence in support of an open-system behavior of the fluid phase, such as highly variable and irregular patterns of oscillatory zoning, could be found. Where oscillatory zoning occurs, the number of oscillations and their relative changes in composition are the same throughout that sample, and may even be correlated between samples collected many kilometers apart.

Keywords: garnet, oscillatory zoning, regional metamorphism, elemental X-ray-intensity mapping (MAPS analysis), Erzgebirge, Germany.

Sommaire

Les schémas de zonation acquis lors de la croissance de cristaux de grenat provenant d'échantillons de l'unité de phyllite à grenat et de l'unité de schiste micacé – eclogite, dans l'Erzgebirge occidental, en Saxe (Allemagne), ont fait l'objet d'une étude détaillée avec une microsonde électronique. Nous nous sommes servis de cartes montrant la répartition d'intensité de raies spécifiques pour certains éléments (analyse MAPS), et d'analyses chimiques quantitatives. Les cristaux zonés de grenat des échantillons de phyllite font preuve d'une diminution progressive dans la teneur en spessartine du coeur (28%, base molaire) vers la bordure (19%), et, à environ 100 μm de la bordure, une oscillation discontinue impliquant une augmentation, une diminution, suivie d'une seconde augmentation, jusqu'à 30%. Ces changements montrent une corrélation avec une zonation oscillatoire antithétique d'amplitude comparable impliquant la composante almandine (47% dans le coeur, 56% vers la bordure, et 49% à la limite du grain). Les données disponibles portant sur la diffusion dans la structure du grenat font penser qu'il n'y aurait pas eu de modification importante de cette zonation de croissance attribuable à une diffusion intracristalline. Dans deux échantillons de schiste micacé, la zonation oscillatoire par rapport à la composante grossulaire montre une corrélation antithétique avec la zonation

[1] *E-mail address*: r.schumacher@uni-bonn.de

en almandin (par exemple, dans l'échantillon E 514: la composante grossulaire atteint 17.0% dans le coeur, diminue jusqu'à 4.7%, augmente jusqu'à 6.8%, et ensuite diminue de nouveau jusqu'à 4.3% à la bordure du grain). Quoique les schémas de zonation par eux-mêmes ne révèlent pas de signes d'une modification après la croissance, les données sur la diffusion ne permettent pas d'écarter complètement cette possibilité. En accord avec les relations texturales observées, nous attribuons les changements oscillatoires en composition du grenat à des réactions continues spécifiques au cours d'un métamorphisme régional. Il y aurait donc eu une évolution complexe impliquant croissance suivie de résorption à cause de variations à courte échelle du taux de décompression des roches. Nous ne voyons aucune évidence pour étayer l'hypothèse d'un système ouvert impliquant une phase fluide, par exemple des schémas de zonation oscillatoire fortement variables et irréguliers. Dans les roches où il y a zonation oscillatoire, le nombre d'oscillations et les changements relatifs en composition sont les même partout dans un échantillon, et pourraient même montrer une corrélation d'un échantillon à l'autre séparés de plusieurs kilomètres.

(Traduit par la Rédaction)

Mots-clés: grenat, zonation oscillatoire, métamorphisme régional, cartes de distribution d'intensité de rayons X (analyse MAPS), Erzgebirge, Allemagne.

Introduction

Patterns of compositional zonation in garnet can give important information on the metamorphic history of a rock. In general, changes in composition from core to rim are characterized by a continuous decrease or increase in a component, with a possible reversal of the trend of some components at the rim due to late consumption or retrograde resorption of the garnet. Less common is oscillatory zoning, which has been reported from open-system environments (*e.g.*, Jamtveit 1991, Jamtveit & Andersen 1992, Jamtveit *et al.* 1993), but seems to be almost unknown from regional metamorphic garnet (Yardley *et al.* 1991).

The samples discussed here are from the regionally metamorphosed Garnet-Phyllite Unit and Mica-Schist/Eclogite Unit of the Western Erzgebirge in Germany (Fig. 1). Grains of garnet in the phyllites and mica schists show zoning with either a continuous decrease or increase in composition from core to rim, as well as rare occurrences of oscillatory zoning in rims about 100 μm wide. We focus here on three examples of oscillatory zoning. We (1) illustrate two types of zoning patterns, (2) discuss the P–T conditions of garnet formation, (3) interpret the zoning in the light of formation due to specific metamorphic reactions and the information thus derived on small-scale variations of the P–T trajectory, and (4) test the possibility of subsequent modification of garnet zoning due to intracrystalline diffusion.

Summary of Geological Setting

The Erzgebirge is a SW–NE-striking anticlinorium predominantly composed of metamorphic rocks covering an area about 50 × 100 km^2. The terrane is situated in the eastern part of the Saxothuringian zone in the Central European Variscides (Fig. 1).

In earlier studies, the various rock units were considered either to be part of a pile of nappes (*e.g.*, Kossmat 1925) or, alternatively, part of a concordant autochthonous succession (*e.g.*, Lorenz & Hoth 1964, 1990). According to the latter lithostratigraphic concept, the Erzgebirge complex preserves its original stratigraphic sequence of Paleozoic to Proterozoic rocks, later intruded by synkinematic granitic intrusions. Krentz (1984) determined P–T conditions of amphibolite-facies metamorphism for the middle and western part of the Erzgebirge.

Structural, petrological, geochemical and geochronological work since 1990 has clearly shown that the Erzgebirge is composed of several metamorphic units with contrasting P–T histories. These units were juxtaposed during exhumation as a result of extensional tectonics (Willner *et al.* 1994, 1997, Rötzler 1995, Krohe 1996, Rötzler *et al.* 1998) to form a large-scale antiform in which the units are now exposed in concentric onion-skin fashion. The contacts between the units are subparallel to a pervasive transposition-induced foliation that represents the dominant structural fabric of the whole structure. In part, these contacts conform to those expected in the formerly accepted lithostratigraphic model; however, the units have been redefined by Willner *et al.* (1994, 1997), Rötzler (1995) and Rötzler *et al.* (1998). From core to rim, these units are the Red- and Grey-Gneiss Unit, the Gneiss/Eclogite Unit, the Mica-Schist/Eclogite Unit, the Garnet-Phyllite Unit and the Phyllite mantle. The three outermost units, the Mica-Schist/Eclogite Unit, the Garnet-Phyllite Unit and the Phyllite mantle, are exposed in the Western Erzgebirge (Fig. 1). For an up-to-date summary of these rock-types, see Willner *et al.* (1997) and Rötzler *et al.* (1998).

Detailed petrological work so far has been carried out on eclogites, gneisses, mica schists and phyllites, with emphasis placed on the geothermobarometry and interpretation of successively formed mineral assemblages within single samples to determine their P–T–t paths (*e.g.,* Schmädicke *et al.* 1992, Massonne 1992, 1994, Rötzler 1995, Willner *et al.* 1994, 1997, Rötzler *et al.* 1998). A summary of P–T paths for the Mica-Schist/Eclogite Unit, the Garnet-Phyllite Unit and the Phyllite Mantle after Rötzler *et al.* (1998) is shown in Figure 2.

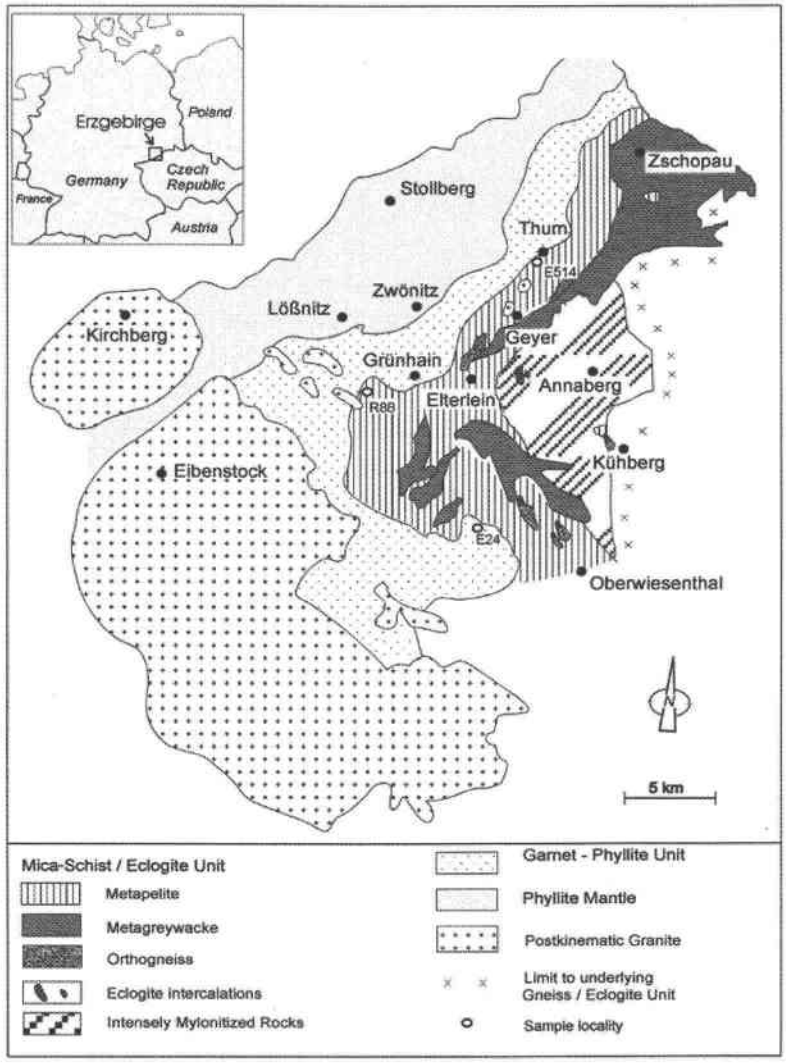

FIG. 1. Simplified geological map of the Western Erzgebirge (location of the Erzgebirge is shown in the inset). Numbers refer to sample localities discussed in the text: garnet phyllite E 24B, mica schist E 514 and mica-schist borehole sample R 88 from a depth of 88 m.

Lenses of eclogite occur throughout the Erzgebirge, but yield different P–T conditions of equilibration. Pressures of up to 27 kbar and temperatures of 800°C of eclogites in the Gneiss/Eclogite Unit are systematically higher than the P–T conditions of 23 kbar and 550°C in the Mica-Schist/Eclogite Unit (Schmädicke *et al.* 1992, Massonne 1992, 1994). Pressures derived from the gneisses and mica schists enclosing the eclogites are also systematically higher in the Gneiss/Eclogite Unit than in the Mica-Schist/Eclogite Unit (Rötzler 1995, Willner *et. al.* 1994, 1997, Rötzler *et al.* 1998). These systematic differences suggest that the two units could have been metamorphosed during the same collision event, but at different depths. On a local scale, the pressures determined for the gneisses and mica schists are also systematically lower than for the enclosed eclogite lenses, but these more felsic rock-types may have re-equilibrated at a lower pressure. An argument for a common subduction history of both rock types is suggested by Rötzler (1997), who interpreted the occurrence of Ba-enriched eclogites next to Ba-enriched metasediments as due to mobilization of Ba caused by dehydration re-

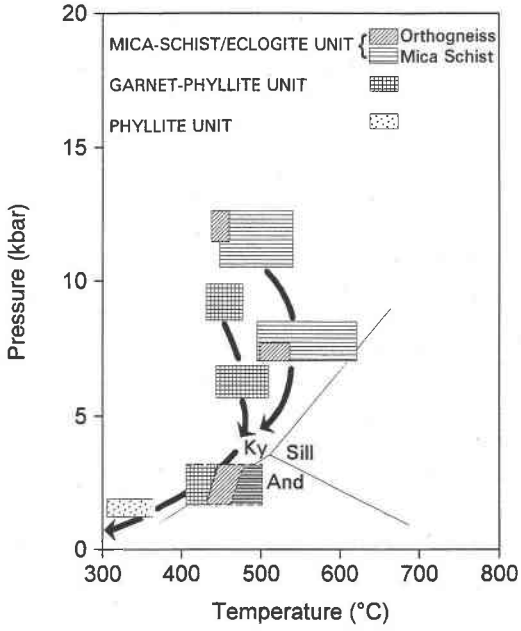

FIG. 2. Summary of P–T paths for the Mica-Schist/Eclogite Unit, the Garnet-Phyllite Unit and the Phyllite Mantle, after Rötzler *et al.* (1998). P–T boxes are based on the analysis of numerous samples.

actions during subduction. In the eclogites, the Ba is incorporated in a barian mica. The fact that the barian mica is preserved as inclusions in garnet indicates that it formed during prograde metamorphism.

There are few age determinations on rocks from the Western Erzgebirge. A lower limit on the age of metamorphism can be derived from the postkinematic granites (Fig. 1). The most recently obtained U–Pb ages on monazite yield about 320 Ma (B. Hansen, Göttingen, pers. commun.). Rb–Sr whole-rock determinations on other discordant granites from the Western Erzgebirge indicate an age of 324 Ma (Gerstenberger 1989).

So far, ages for the climax of metamorphism in the Western Erzgebirge are lacking. Pb–Pb ages of metamorphic zircon from quartzofeldspathic rocks of the Gneiss/Eclogite Unit (Central Erzgebirge) yield about 340 Ma (Kröner & Willner 1995, Kotková *et al.* 1996, Willner *et al.* 1996). However, since the closure temperature of zircon probably lies below the maximum temperatures of metamorphism, which exceeded 700°C, the zircon ages could also indicate minimum ages. Despite these uncertainties, the age data on the postkinematic granites (about 320 Ma) and the quartzofeldspathic rocks (about 340 Ma) point to a cooling interval of about 20 Ma, a time span important for later discussions of the cooling history of the garnet from this study.

Schmädicke *et al.* (1995) determined an age of 360 ± 7 Ma from Sm–Nd garnet – clinopyroxene – whole-rock isochron data on an eclogite of the same unit. This age was interpreted to be the most reliable age of high-P metamorphism for the eclogites. These authors also presented ^{40}Ar–^{39}Ar ages of 348 ± 2 and 355 ± 2 Ma for phengite from two eclogites and, from the similarity of the Sm–Nd and the ^{40}Ar–^{39}Ar ages, deduced a minimum cooling rate of about 50°C Ma^{-1}.

Analytical Methods

The minerals of the samples were quantitatively analyzed with one of two electron microprobes, a JEOL 8600 MX Superprobe at the University of Münster and a Cameca SX–50 microprobe at the GeoForschungs-Zentrum in Potsdam. Operating conditions were 15 kV accelerating voltage, beam current of 15 nA or 20 nA, and measuring time of 20 seconds on the peak and 10 seconds on the background on each side. Abbreviations of minerals are those of Kretz (1983), and representative results of chemical analyses are given in Table 1. The mineral formulae were calculated on the basis of a fixed number of oxygen atoms (garnet, ilmenite, white mica, biotite, chlorite, plagioclase) or, in order to calculate the ferric iron contents, on the basis of a fixed number of oxygen atoms and cations (clinozoisite). The garnet typically has a cation sum of somewhat less than 8 atoms per formula unit (*apfu*), and ilmenite, less than 2 *apfu*, indicating that no ferric iron is present. To avoid possible errors introduced by differences between the electron microprobes, analytical results that were used for a geothermobarometric calculation were all obtained at the same facility.

In addition to quantitative electron-microprobe analyses, X-ray element intensity mapping (MAPS) of selected elements was carried out with a JEOL 8600 MX Superprobe at the University of Münster and a Cameca SX–50 microprobe at the University of Bochum using wavelength-dispersion spectrometers across up to 2 × 2 mm large areas of garnet, plagioclase and surrounding minerals. The X-ray intensities of Mn, Ca, Fe and Mg were measured with pixel sizes of 2 to 5 μm^2. This technique is a very sensitive method for determining patterns of zoning and reveals considerably more information than line traverses across the grains.

Types of Garnet Zoning

With the help of the MAPS approach, we were able to distinguish the following core-to-rim patterns of zoning in grains of garnet from the Western Erzgebirge: (1) Continuous, monotonic zoning is shown by most grains in the garnet phyllites and the mica schists. Almandine and pyrope components increase, whereas spessartine and grossular components decrease from core to rim. Retrograde zoning at the rim is usually characterized by an increasing proportion of spessartine and reduction in

TABLE 1. REPRESENTATIVE COMPOSITIONS OF MINERALS IN PHYLLITES AND MICA SCHISTS OF THE WESTERN ERZGEBIRGE, GERMANY

	E 24B Garnet									E 24B Clinozoisite	
Anal.#	1 rim MAPS high-Mn	2 MAPS	5 MAPS low-Mn	B9 MAPS high-Mn	B13 MAPS low-Mn	11 core MAPS	6 MAPS next to Ilm 55	183 core high-Mn	K21 incl. in Ab blast		K20 incl. in Ab blast
SiO_2 wt%	37.14	37.10	37.11	37.01	36.76	36.98	37.35	38.28	37.29	SiO_2	38.68
TiO_2	0.23	0.11	0.08	0.06	0.08	0.22	0.11	0.16	0.08	TiO_2	0.37
Al_2O_3	21.08	21.14	21.31	20.68	20.69	20.98	21.08	21.87	20.58	Al_2O_3	25.84
Cr_2O_3	0.07	0.01	0.00	0.00	0.09	0.00	0.00	0.07	0.05	Cr_2O_3	0.14
FeO	22.00	23.64	25.90	25.70	26.43	20.56	23.77	18.83	26.01	Fe_2O_3	7.99
MnO	13.42	10.98	7.21	8.15	7.31	12.02	9.11	16.81	6.70	FeO	0.07
MgO	0.62	0.56	0.43	0.37	0.41	0.33	0.46	0.19	0.41	MnO	0.17
CaO	6.57	6.43	8.22	7.94	8.19	8.36	8.46	6.64	8.26	MgO	0.06
Na_2O				0.00						CaO	23.73
K_2O				0.00						Na_2O	0.00
Total	101.13	99.97	100.26	99.91	99.96	99.45	100.34	102.85	99.38	Total	97.05
Si *apfu*	2.977	2.997	2.984	2.998	2.980	2.994	3.006	3.003	3.023	Si	3.041
Al	1.991	2.013	2.020	1.974	1.977	2.002	1.989	2.022	1.966	Al	2.394
Ti	0.014	0.007	0.005	0.004	0.005	0.013	0.007	0.009	0.005	Ti	0.022
Cr	0.004	0.001	0.000	0.000	0.006	0.000	0.000	0.004	0.003	Cr	0.009
Fe^{3+}										Fe^{3+}	0.473
Mg	0.074	0.067	0.052	0.045	0.049	0.040	0.055	0.023	0.050	Mg	0.007
Fe^{2+}	1.475	1.597	1.742	1.741	1.792	1.392	1.592	1.235	1.763	Fe^{2+}	0.045
Mn	0.911	0.751	0.491	0.559	0.502	0.824	0.618	1.117	0.460	Mn	0.011
Ca	0.564	0.557	0.708	0.689	0.712	0.725	0.726	0.558	0.717	Ca	1.999
Na										Na	0.000
K										K	0.000
Sum	8.010	7.990	8.002	8.010	8.023	7.990	7.993	7.971	7.987	Sum	8.001
X_{Mg}	0.048	0.040	0.029	0.025	0.027	0.028	0.033	0.018	0.028		
Alm	48.8	53.7	58.2	57.4	58.7	46.7	53.2	42.1	59.0		
Grs	18.7	18.7	23.7	22.7	23.3	24.3	20.7	19.0	24.0		
Prp	2.4	2.3	1.7	1.5	1.6	1.3	1.8	0.8	1.7		
Sps	30.1	25.3	16.4	18.4	16.4	27.7	24.3	38.1	15.4		

The structural formula of garnet is based on twelve atoms of oxygen. That of clinozoisite is based on eight cations and 12.5 atoms of oxygen. $X_{Mg} = Mg/(Mg + Fe^{2+})$. The proportion of cations is expressed in *apfu*, atoms per formula unit.

the almandine and grossular components. (2) Oscillatory changes in almandine and spessartine or almandine and grossular components have been found within the outermost edge of garnet grains from three out of about 30 samples. The samples are labeled E 24B, E 514 and R 88 (Figs. 3, 4, 5 and 6; localities are given in Fig. 1). Several grains from each sample have been investigated with the MAPS method.

Textures of Samples, Mineral Assemblages and Mineral Composition

Of the three samples with oscillatory zoning, garnet phyllite E 24B from locality E 24 and mica schist E 514 will be discussed in detail.

A detailed discussion of the rock textures has been presented by Rötzler *et al.* (1998), so that only a brief summary is given here. Three phases of deformation can be differentiated; they are best illustrated by the compositions and textures of the coeval generations of white mica: (1) relics of the s_1 schistosity included in garnet and albite and in pressure shadows of porphyroblasts; in these, white mica (WM I) is phengitic, with Si-contents up to 3.4 *apfu* in phyllite and 3.55 *apfu* in mica schist; (2) phengitic white mica forming the predominant schistosity s_2 (WM II with Si of about 3.2 to 3.3 *apfu* in both rock types) and (3) muscovite in late s_3 microshear zones with low Si contents (WM III with Si of 3.00 to 3.15 *apfu*) (Table 1).

TABLE 1 (cont.). REPRESENTATIVE COMPOSITIONS OF MINERALS IN PHYLLITES AND MICA SCHISTS OF THE WESTERN ERZGEBIRGE, GERMANY

	E 24B Ilmenite					E 24B White mica				
Anal #	55 incl. in Grt	59 incl. in Grt	67 matrix, rim	68 matrix, core		88 WM I core, matrix	K18 WM I incl. in Ab blast	74 WM II core, matrix	78 WM III rim, matrix	49 WM III in shear zone
SiO_2 wt%	0.10	0.08	0.16	0.06	SiO_2	52.84	52.95	50.28	47.92	46.32
TiO_2	51.49	53.69	53.92	54.11	TiO_2	0.25	0.20	0.27	0.29	0.32
Al_2O_3	0.04	0.03	0.10	0.00	Al_2O_3	28.48	29.87	31.81	34.63	36.00
Cr_2O_3	0.00	0.00	0.03	0.00	Cr_2O_3	0.04	0.05	0.00	0.00	0.00
FeO	42.97	40.48	38.85	39.91	FeO	3.62	3.65	2.72	1.74	1.93
MnO	2.57	6.72	7.64	6.53	MnO	0.04	0.00	0.03	0.00	0.08
MgO	0.15	0.00	0.02	0.00	MgO	2.43	2.15	1.56	0.83	0.93
CaO	0.23	0.21	0.03	0.00	CaO	0.00	0.00	0.00	0.02	0.01
Na_2O	0.00	0.00	0.01	0.00	Na_2O	0.22	0.14	0.53	0.44	0.41
K_2O	0.00	0.00	0.13	0.07	K_2O	9.80	7.66	9.86	9.60	9.61
Total	97.55	101.21	100.89	100.68	Total	97.72	96.67	97.06	95.47	95.61
Si *apfu*	0.003	0.002	0.004	0.001	Si	3.427	3.419	3.280	3.160	3.062
Al	0.001	0.001	0.003	0.000	Al	2.177	2.273	2.445	2.692	2.805
Ti	0.999	1.003	1.007	1.014	Ti	0.012	0.010	0.013	0.015	0.016
Fe^{3+}					Fe^{3+}					
Mg	0.006	0.000	0.001	0.000	Mg	0.235	0.207	0.152	0.082	0.092
Fe^{2+}	0.927	0.841	0.807	0.831	Fe^{2+}	0.196	0.197	0.148	0.096	0.107
Mn	0.056	0.141	0.161	0.138	Mn	0.002	0.000	0.001	0.000	0.004
Ca	0.006	0.005	0.001	0.000	Ca	0.000	0.000	0.000	0.001	0.001
Na	0.000	0.000	0.000	0.000	Na	0.027	0.018	0.067	0.057	0.053
K	0.000	0.000	0.004	0.002	K	0.811	0.631	0.820	0.808	0.811
Sum	1.998	1.993	1.989	1.986	Sum	6.890	6.758	6.926	6.912	6.951
X_{Mn}	0.060	0.143	0.166	0.142						

The structural formula of ilmenite is based on three atoms of oxygen. That of white mica is based on eleven atoms of oxygen. $X_{Mn} = Mn/(Mn + Mg + Ca + Fe^{2+})$.

In a few mica schists from other localities, relics of early albite (Pl I) formed at the highest pressure of metamorphism are found as inclusions in garnet. Later plagioclase of oligoclase composition (Pl II in Table 1) was largely consumed (Rötzler 1995) by a still younger generation of albite porphyroblasts (Pl III), which have an An-enriched rim (Fig. 7, Pl IV in Table 1). These porphyroblasts are cut by s_3 microshear zones and formed during decompression.

Sample E 24B: phyllite from the Garnet-Phyllite unit

Sample E 24B is a Mn-rich phyllite from the Garnet-Phyllite Unit with the mineral assemblage garnet + white mica + biotite + chlorite + clinozoisite (absent in the matrix) + albite + ilmenite + quartz + rutile. The albite porphyroblasts (Pl III) contain inclusions of fine-grained garnet, white mica with Si-contents of up to 3.4 *apfu* (WM I), biotite, chlorite, clinozoisite and ilmenite (Fig. 8a). In the matrix, garnet forms euhedral porphyroblasts up to 0.6 mm in diameter (Fig. 8b), with inclusions of ilmenite, rutile, quartz and chlorite. The white mica of the matrix (WM II or III) generally contains less Si than the inclusions in the albite porphyroblasts (WM I, Table 1). In general, WM I and WM II–III are distinguished on the basis of textural relations. However, the cores of phengitic white mica from the matrix and grains that grew in pressure shadows also show high Si contents (WM I). Chlorite occurs as inclusions in albite and, less commonly, garnet porphyroblasts, as a matrix phase, and as a late, Fe-rich secondary product forming at the expense of garnet. Clinozoisite is absent in the matrix, and most likely was consumed together with early chlorite during garnet growth. After consumption of clinozoisite and some chlorite, an early plagioclase of oligoclase composition and further chlorite could have reacted to form the albite porpyroblasts and enabled further growth of garnet. Relics of this type of oligoclase were found in some mica schists, but not in the garnet phyllite.

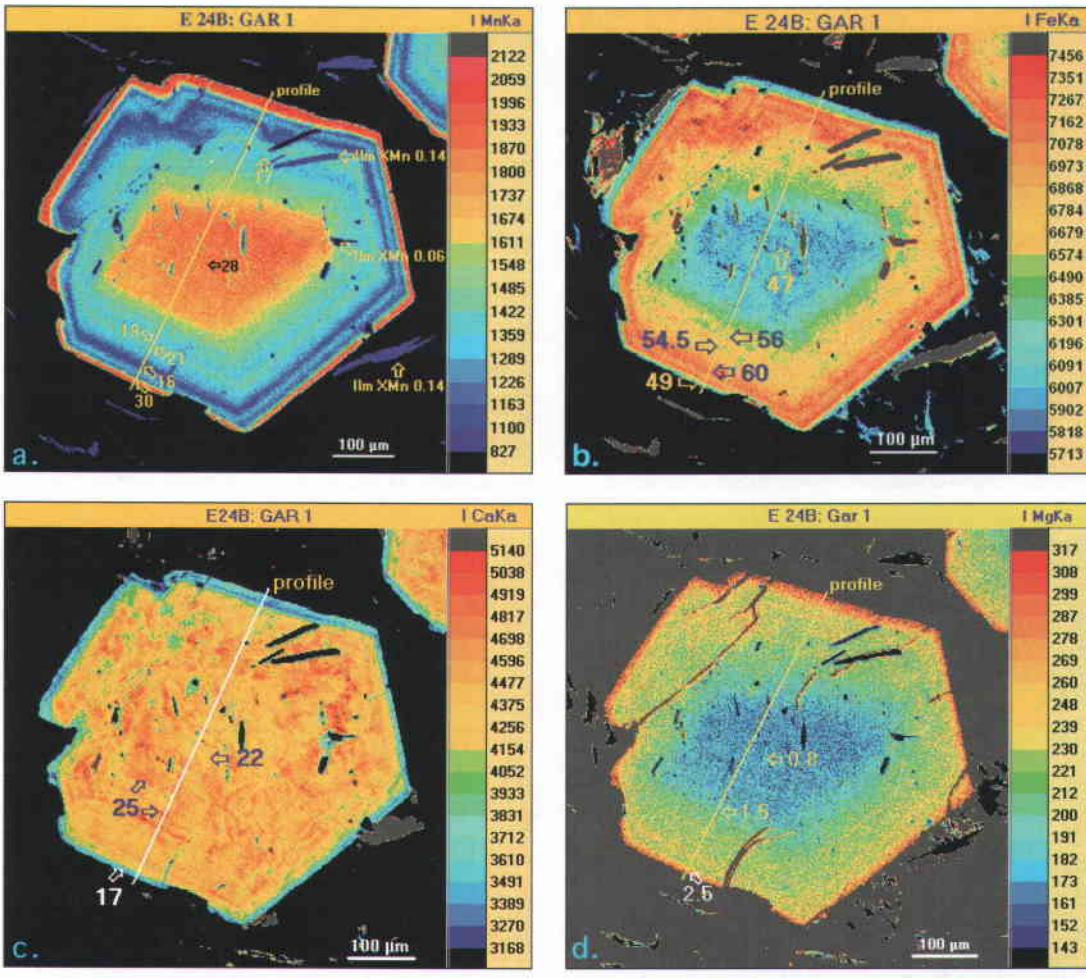

FIG. 3. MAPS analysis of a garnet porphyroblast from garnet phyllite E 24B (see thin-section sketch of textural relationships in Fig. 8b). Colors indicate areas of similar X-ray intensities; numbers indicate mole % of the spessartine component (a), the almandine component (b), the grossular component (c) and the pyrope component (d). Line across the grain indicates location of profile with quantitative analyses (Fig. 9).

Garnet in sample E 24B shows a continuous decrease in the spessartine component from the core (*e.g.*, 28 mole % Sps) toward the rim (*e.g.*, 19 mole % Sps) and, over about 100 µm at the rim, an oscillatory increase, decrease and further increase (*e.g.*, 30 mole % Sps) (Figs. 3a and 9). An additional narrow zone showing a decrease may occur close to the outermost rim (Fig. 3a). The oscillatory pattern conforms to the euhedral outline of the crystal. The variations in spessartine content are correlated with antithetic changes in almandine content of comparable magnitude (*e.g.*, $Alm_{47} \rightarrow Alm_{56} \rightarrow Alm_{49}$ from core to rim). Although an antithetic oscillatory pattern is present (Figs. 3b, 9), this feature is less obvious in some parts of the grain for almandine than for spessartine in the MAPS analyses (Fig. 3), because the higher absolute amounts of almandine lead to a smaller relative change in the compositional oscillations.

The grossular component shows a significant decrease at the outermost rim (Figs. 3c, 9). The pyrope component increases only very slightly from core to rim (Figs. 3d, 9), so that the almandine content dictates X_{Mg}, which decreases outward from the core but increases near the rim (Fig. 3b, Table 1).

Ilmenite is a common phase in the matrix and as inclusions in the albite and garnet porphyroblasts (Figs. 8a, b). The inclusions are difficult to analyze, because usually only very small domains are actually exposed

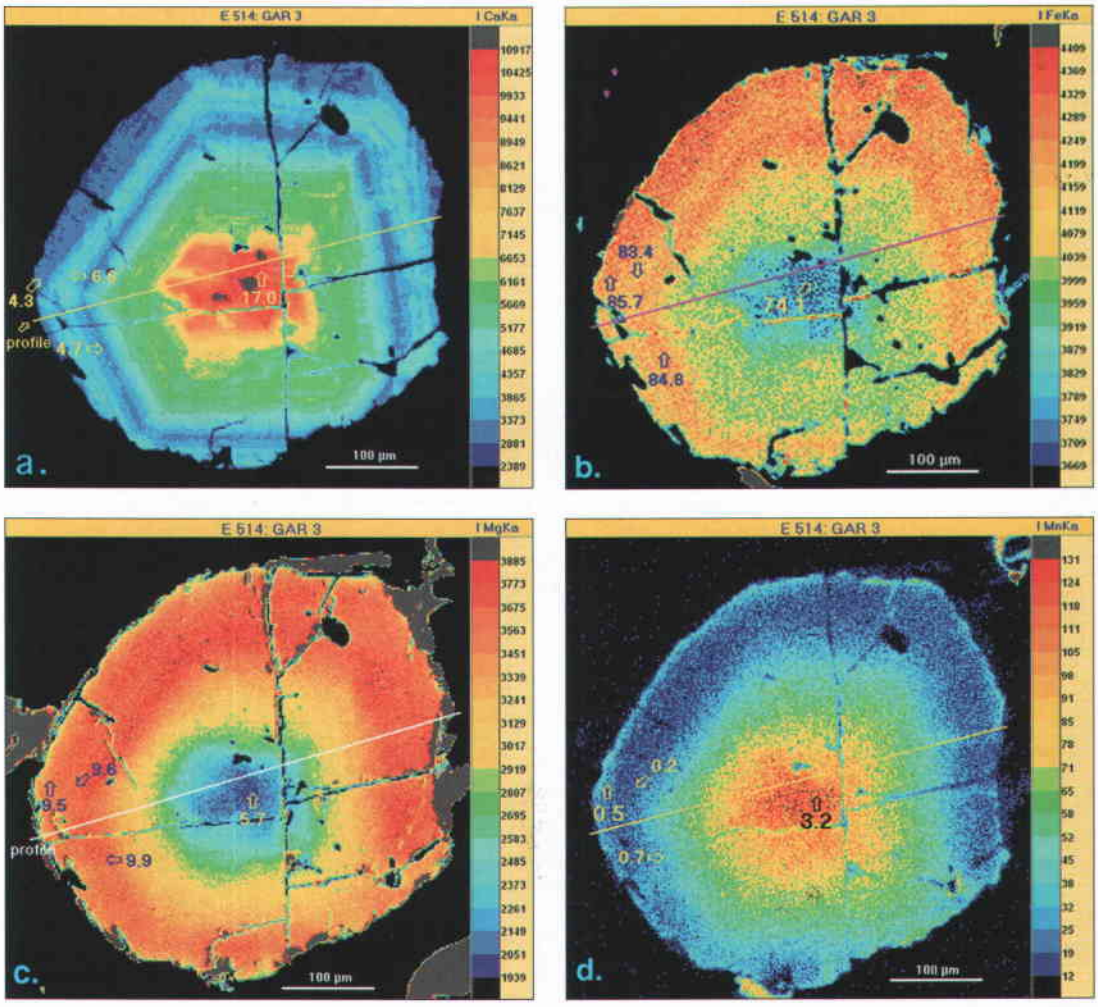

FIG. 4. MAPS analysis of a grain of garnet from mica schist E 514. Colors indicate areas of similar X-ray intensities; numbers indicate mole % of the grossular component (a), the almandine component (b), the pyrope component (c) and the spessartine component (d). Line across the grain indicates location of profile with quantitative analyses (Fig. 12).

on the polished surface. Consequently, most quantitative analyses are found to represent mixtures of two phases. Some acceptable analyses of ilmenite inclusions from within garnet show variable Mn-contents (Table 1), with ilmenite from the inner Mn-rich garnet zone being poorer in Mn (*e.g.*, Ilm 55 with 2.57 wt. % MnO, X_{Mn} = 0.06, Table 1) than that from the outer zones (*e.g.*, Ilm 59 with 6.72 wt. % MnO, X_{Mn} = 0.14, Table 1). Compositions of the Mn-rich ilmenite included in the outer zones of the garnet correspond those of the matrix ilmenite (Table 1). The ilmenite inclusions close to the garnet core are so distinctly different in composition that they may represent detrital grains overgrown by garnet.

Samples E 514 and R 88: garnet-bearing mica schists from the Mica-Schist/Eclogite unit

Sample E 514 contains the mineral assemblage garnet + white mica + biotite (accessory) + chlorite + plagioclase + quartz + ilmenite + rutile + tourmaline. Some samples from this locality may contain the critical assemblage garnet – chloritoid – biotite rather than garnet – chlorite – biotite. As discussed by Rötzler *et al.* (1998), this difference may be due to variations in bulk-rock composition, the chloritoid-bearing samples being more aluminous.

The three generations of white mica have Si = 3.5–3.4 (WM I), Si = 3.3–3.2 (WM II) to 3.1 *apfu* (WM III)

TABLE 1 (cont.). REPRESENTATIVE COMPOSITIONS OF MINERALS IN PHYLLITES AND MICA SCHISTS OF THE WESTERN ERZGEBIRGE, GERMANY

	E 24B Biotite				E 24B Chlorite			E 24B Albite porphyroblast	
Anal.#	92 next to Grt	K12 matrix	K17 incl. in Ab		116 incl. in Ab	146 incl. in Ab blast	163 matrix		139
SiO_2 wt%	45.85	35.21	34.96	SiO_2	25.25	25.14	24.96	SiO_2	69.73
TiO_2	0.90	2.03	1.70	TiO_2	0.15	0.08	0.17	TiO_2	0.00
Al_2O_3	16.67	17.32	16.64	Al_2O_3	23.03	21.79	21.34	Al_2O_3	19.82
Cr_2O_3	0.00	0.03	0.25	Cr_2O_3	0.07	0.01	0.02	Cr_2O_3	0.00
FeO	19.16	24.07	24.48	FeO	23.88	30.92	29.23	FeO	0.02
MnO	0.32	0.28	0.29	MnO	0.35	0.52	0.39	MnO	0.00
MgO	7.24	6.39	6.82	MgO	16.04	10.69	11.22	MgO	0.00
CaO	0.00	0.00	0.00	CaO	0.00	0.01	0.01	CaO	0.07
Na_2O	0.05	0.06	0.04	Na_2O	0.03	0.02	0.02	Na_2O	11.37
K_2O	8.09	9.56	9.72	K_2O	0.13	0.01	0.02	K_2O	0.10
Total	98.28	94.95	94.90	Total	88.93	89.19	87.38	Total	101.11
Si *apfu*	3.258	2.763	2.760	Si	2.604	2.683	2.699	Si	3.004
Al	1.396	1.602	1.548	Al	2.799	2.740	2.720	Al	1.006
Ti	0.048	0.120	0.101	Ti	0.012	0.006	0.014	Ti	0.000
Cr	0.000	0.002	0.016	Cr	0.006	0.001	0.002	Cr	0.000
Fe^{3+}				Fe^{3+}				Fe^{3+}	
Mg	0.767	0.748	0.803	Mg	2.059	1.700	1.809	Mg	0.000
Fe^{2+}	1.138	1.580	1.616	Fe^{2+}	2.466	2.759	2.643	Fe^{2+}	0.001
Mn	0.019	0.019	0.019	Mn	0.031	0.047	0.036	Mn	0.000
Ca	0.000	0.000	0.000	Ca	0.000	0.001	0.001	Ca	0.003
Na	0.007	0.009	0.006	Na	0.006	0.004	0.004	Na	0.950
K	0.734	0.957	0.979	K	0.018	0.001	0.003	K	0.005
Sum	7.367	7.800	7.848	Sum	10.001	9.942	9.931	Sum	4.970
X_{Mg}	0.403	0.321	0.332	X_{Mg}	0.455	0.381	0.406		

The structural formula of biotite is based on eleven atoms of oxygen. That of chlorite is based on fourteen atoms of oxygen, and that of albite, on eight atoms of oxygen. $X_{Mg} = Mg/(Mg + Fe^{2+})$.

(Table 1). Garnet occurs as inclusions in albite porphyroblasts (Fig. 10) and in the matrix. Rare biotite occurs in the matrix. Relict chlorite forms inclusions in garnet, whereas a late generation of chlorite poorer in Fe and Al is found enclosed in the An-enriched rim of the albite porphyroblasts (Fig. 11) and as a reaction product surrounding corroded grains of garnet. Relict oligoclase (Pl II) occurs in the matrix. Albite porphyroblasts are predominant (Pl III) and have an An-enriched rim (Pl IV, Fig. 10). The X-ray element intensity maps show slight, but systematic variations in the composition of the albite porphyroblasts and the An-enriched rim (Fig. 7).

In samples of mica schist, the oscillatory zoning in garnet is characterized by a pronounced decrease, increase, decrease and then another increase of the grossular component, which correlates with an antithetic zoning of the almandine component (Figs. 4, 12). While preparing the final figures for publication with enhanced resolution, it was discovered that at least one more minor feature (increase and decrease in grossular component) may be superimposed on the zoning at a distance of about 150 μm from the rim (Figs. 4a, 12). This feature does not modify the conclusion reached; in fact it strengthens the argument that post-growth modification has not occurred. As in the garnet phyllite, the *relative* variations in almandine are smaller, and color variations in the MAPS analysis are therefore less distinct. An example of the zoning in sample E 514 gave $Alm_{74.1}$ $Grs_{17.0}$ $Prp_{5.7}Sps_{3.2}$ in the core (Figs. 4a–d). At the rim, the grossular component oscillates between 4.3 and 6.8 mole % (Fig. 4a), with an antithetic zoning of the almandine component between 85.7 and 83.4 mole % (Fig. 4b). The Ca pattern is euhedral, with the exception of the outermost zone of garnet in contact with the matrix (Fig. 4). There, the corroded appearance of the rim and an increase in spessartine component point to a garnet-consuming reaction. Similar oscillatory zoning with respect to Ca with the same number of major zones is found in garnet from sample R88 (Fig. 6). Since the

TABLE 1 (cont.). REPRESENTATIVE COMPOSITIONS OF MINERALS IN PHYLLITES AND MICA SCHISTS OF THE WESTERN ERZGEBIRGE, GERMANY

	E 514 Garnet				E 514 Ilmenite			E 514 White mica			
Anal #	21 rim (MAPS) 1. low-Ca	B7 (MAPS) 1. high-Ca	B14 (MAPS) 2. low-Ca	33 core (MAPS) 2. high-Ca		50 incl. in Ab		18(1) WM I matrix	24(2) WMI pressure shadow	14(2) WM II matrix	34(2) WM III shear zone
SiO_2 wt%	37.12	36.84	36.72	37.03	SiO_2	0.05	SiO_2	49.48	50.99	47.87	47.40
TiO_2	0.05	0.05	0.03	0.06	TiO_2	56.34	TiO_2	0.29	0.40	0.38	0.11
Al_2O_3	20.81	21.19	21.05	20.94	Al_2O_3	0.01	Al_2O_3	35.32	28.49	31.88	36.23
Cr_2O_3	-	0.00	0.00	0.02	Cr_2O_3	0.00	Cr_2O_3	0.01	0.00	0.03	0.02
FeO	36.31	38.44	38.64	32.49	FeO	44.32	FeO	1.31	2.71	2.05	0.79
MnO	0.20	0.07	0.29	1.39	MnO	1.21	MnO	0.04	0.00	0.00	0.01
MgO	2.27	2.48	2.53	1.39	MgO	0.03	MgO	0.79	2.59	1.42	0.38
CaO	1.43	2.43	1.65	5.83	CaO	0.00	CaO	0.03	0.01	0.00	0.01
Na_2O	0.06	0.00	0.00	0.05	Na_2O	0.00	Na_2O	0.96	0.63	0.83	1.72
K_2O	-	0.00	0.00	0.00	K_2O	0.00	K_2O	7.98	9.61	9.77	8.93
Total	98.25	101.50	100.91	99.20	Total	101.96	Total	96.21	95.43	94.24	95.60
Si *apfu*	3.038	2.952	2.961	3.004	Si	0.001	Si	3.488	3.383	3.219	3.110
Al	2.008	2.002	2.001	2.002	Al	0.000	Al	2.935	2.228	2.526	2.802
Ti	0.003	0.003	0.002	0.003	Ti	1.034	Ti	0.016	0.020	0.019	0.005
Cr	0.000	0.000	0.000	0.002	Cr	0.000	Cr	0.000	0.000	0.001	0.001
Fe^{3+}					Fe^{3+}		Fe^{3+}				
Mg	0.277	0.297	0.305	0.169	Mg	0.001	Mg	0.083	0.256	0.143	0.037
Fe^{2+}	2.485	2.576	2.606	2.204	Fe^{2+}	0.904	Fe^{2+}	0.077	0.150	0.115	0.043
Mn	0.014	0.005	0.020	0.095	Mn	0.025	Mn	0.002	0.000	0.000	0.001
Ca	0.125	0.209	0.143	0.506	Ca	0.000	Ca	0.002	0.001	0.000	0.001
Na	0.009	0.000	0.000	0.008	Na	0.000	Na	0.131	0.081	0.109	0.219
K	-	0.000	0.000	0.000	K	0.000	K	0.718	0.813	0.838	0.748
Sum	7.959	8.044	8.038	7.993	Sum	1.965	Sum	7.453	6.932	6.970	6.967
X_{Mg}	0.100	0.103	0.105	0.071	X_{Mn}	0.027					
Alm	85.7	83.4	84.8	74.1							
Grs	4.3	6.8	4.7	17.0							
Prp	9.5	9.6	9.9	5.7							
Sps	0.5	0.2	0.7	3.2							

The structural formula of garnet is based on twelve atoms of oxygen. That of ilmenite is based on three atoms of oxygen, and that of white mica, on eleven atoms of oxygen. $X_{Mg} = Mg/(Mg + Fe^{2+})$; $X_{Mn} = Mn/(Mn + Mg + Ca + Fe^{2+})$

resolution of this dataset is lower than the one shown in Figure 4, the minor Ca-oscillations nearer the core are not seen.

In all cases of oscillatory zoning, the patterns of zoning are euhedral (spessartine and almandine component in garnet phyllite E 24B; grossular and almandine component in mica schists E 514 and R88), and therefore point to growth zoning. This is especially surprising with respect to sample E 24B, since an increase in the spessartine component at the rim is generally attributed to garnet resorption, during which Mg and Fe are selectively removed, causing Mn to diffuse inward (*e.g.*, Evans & Guidotti 1966, Robinson 1991).

As indicated above, components showing oscillatory zoning are superimposed on others that are zoned monotonically. The grossular and pyrope components in garnet from the garnet phyllite, and the pyrope and spessartine components in garnet from the mica schists, either increase or decrease continuously from core to rim. Possible modification of zoning patterns by intracrystalline diffusion will be addressed below.

P–T Conditions of Garnet Formation

P–T paths for the Garnet-Phyllite Unit and the Mica-Schist/Eclogite Unit have been obtained by Rötzler (1995) and Rötzler *et al.* (1998) by applying conventional thermobarometry as well as the TWEEQU method with the internally consistent thermodynamic dataset of Berman (1988), revised in 1992 (Fig. 2).The

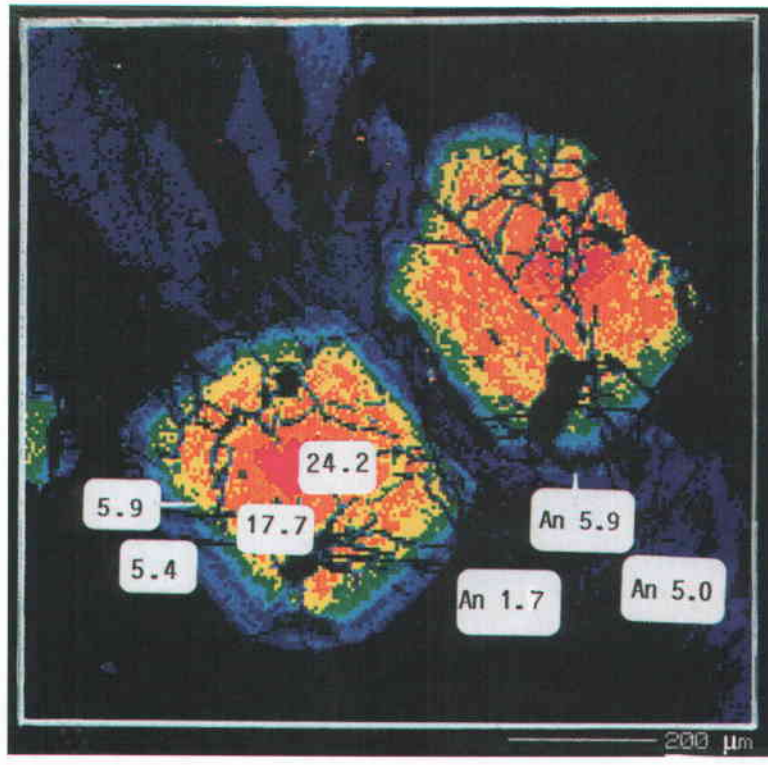

FIG. 5. MAPS analysis of two grains of garnet enclosed in an albite porphyroblast from mica schist E 514. The left-hand grain is fully enclosed by albite; the grain on the right is only half enclosed by the An-enriched rim of the albite porphyroblast, and the other half lies within the sheared matrix (s_3) and is corroded. A thin-section sketch with further textural relationships is given in Figure 10.

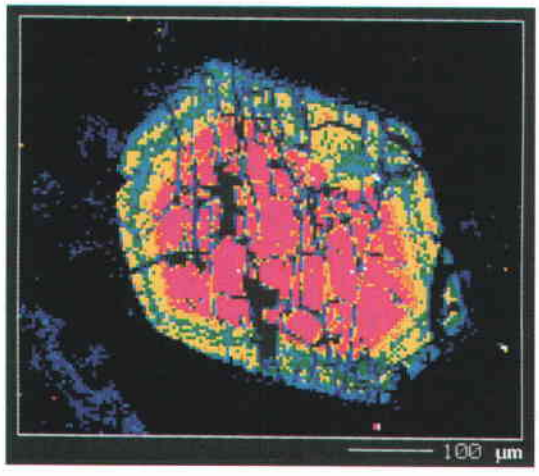

FIG. 6. MAPS analysis of a garnet grain from mica schist R 88. Even though this locality is more than 10 km away from locality E 514, the same number of oscillatory Ca zones are observed.

core to near-rim part of the zoned grains in garnet phyllite E 24B (with decreasing spessartine, increasing almandine, almost constant grossular and slightly increasing pyrope components) are interpreted to have formed under prograde P–T conditions. Continued growth of the rim took place during heating at decreasing pressures. This interpretation is in agreement with P–T data obtained with the TWEEQU method, which is based on a garnet composition from a transitional core–rim area (highest-P conditions?), phengitic white mica (WM I), biotite, chlorite, rutile and ilmenite. Temperatures of about 490°C were reached at a maximum P near 9.7 kbar (Rötzler *et al.* 1998). P–T conditions of about 6 kbar and 500°C were obtained from garnet rim, WM II and albite of a garnet phyllite with grains of garnet that do not show oscillatory zoning.

The outermost rim of garnet grains in sample E 24B, up to 100 µm wide, is interpreted to have grown during decompression and a slight increase in T. The fact that the oscillatory zoning pattern in the garnet shows euhedral outlines, along with an increase in X_{Mg} (Table 1), points to formation during an increase in tem-

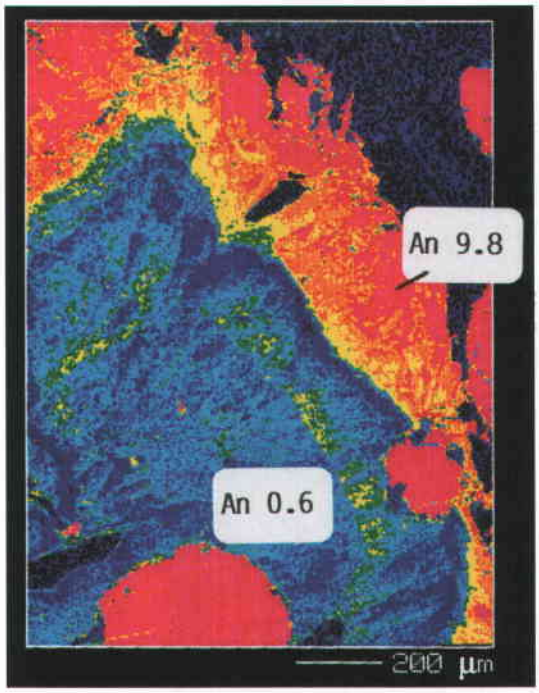

FIG. 7. Typical MAPS analysis of an albite porphyroblast and its An-enriched rim from mica schist E 514. MAPS analysis allows recognition of a Ca-rich growth zone (yellow) in the core and a systematic zonation in the rim (yellow to red). Two enclosed subhedral grains of garnet are recognizable by the uniform red color.

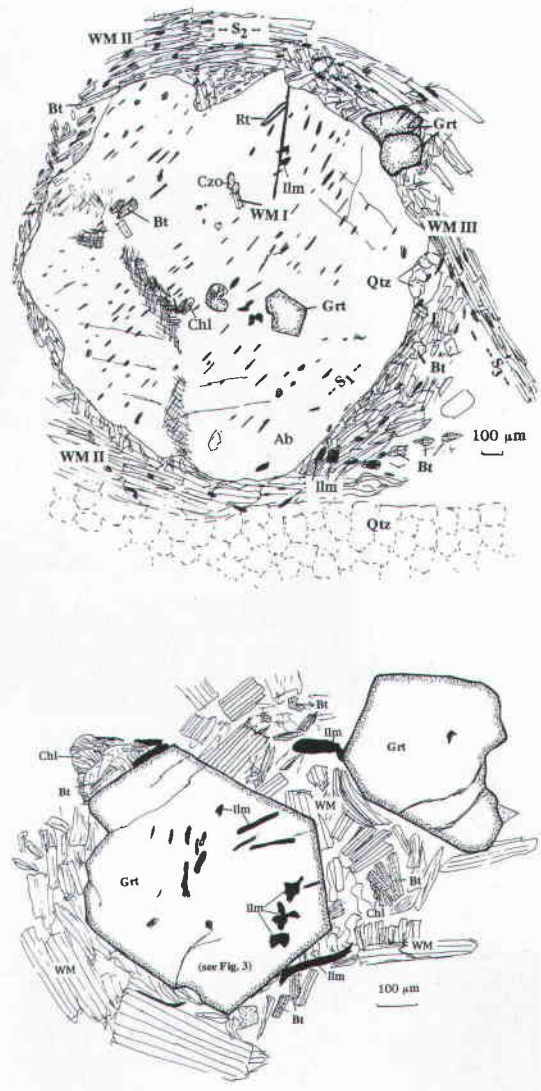

FIG. 8. Sketches of textural relationships in garnet phyllite E 24B: (a) albite porphyroblast with fine-grained inclusions of garnet, clinozoisite, biotite, white mica, chlorite, ilmenite and rutile. The s_2 schistosity is the dominant schistosity of the matrix; the s_3 schistosity forms in micro shear zones. (b) Rock matrix with garnet porphyroblasts, in which ilmenite and rutile are enclosed. Element-distribution maps of the left-hand porphyroblast are shown in Figure 3.

perature. The grossular component remains fairly constant within the core, and decreases at the rim (Figs. 3c, 9), pointing to decreasing pressure.

As described earlier, garnet and ilmenite are the only minerals that contain considerable amounts of Mn (Table 1). Ilmenite included in the outer zones of the garnet could have exchanged Fe and Mn with the garnet, causing the oscillatory patterns of zoning to develop. This may also be indicated by the zones of Mn depletion around ilmenite inclusions in garnet (Fig. 3a). However, the analyzed grains of ilmenite were too small to detect any oscillatory zoning corresponding to that in the garnet. The Fe–Mn exchange equilibrium was used to explore possible variations in temperatures based on the Powneeby *et al.* (1987) Fe–Mn geothermometer for garnet and ilmenite. Application of this thermometer with a correction for the activity of spessartine component after Ganguly & Saxena (1984) yields a large range of mostly unrealistically high temperatures. Compositions obtained from garnet poorer in the spessartine component and ilmenite richer in Mn yield temperatures of up to 1400°C. The calculated temperatures, as well as those obtained from the outermost Mn-rich rim (with up to 30 mole % spessartine component) and matrix ilmenite (with 14 to 17 mole % pyrophanite, $MnTiO_3$, component), are interpreted to be due to disequilibrium (overstepping of the garnet–ilmenite Fe–Mn exchange reaction?).

TABLE 1 (cont.) REPRESENTATIVE COMPOSITIONS OF MINERALS IN PHYLLITES AND MICA SCHISTS OF THE WESTERN ERZGEBIRGE, GERMANY

E 514 Biotite		E 514 Chlorite					E 514 Plagioclase			
Anal.	KR matrix		62 incl. in Grt (early Chl)	39 matrix core	44 incl. in Pl rim	16/2(1) late, from Grt		KR2 Pl II: relic in matrix	57 Pl III: core of Ab	52 Pl IV: rim of Ab
SiO_2 wt%	36.28	SiO_2	24.93	25.00	25.66	24.81	SiO_2	63.49	69.75	68.00
TiO_2	1.85	TiO_2	0.09	0.11	0.08	0.11	TiO_2	0.00	0.00	0.00
Al_2O_3	19.33	Al_2O_3	22.94	22.74	22.34	22.96	Al_2O_3	21.97	19.58	20.58
Cr_2O_3	0.03	Cr_2O_3	0.00	0.05	0.01	0.04	Cr_2O_3	0.00	0.00	0.00
FeO	17.68	FeO	29.03	26.35	26.56	27.87	FeO	0.05	0.01	0.06
MnO	0.07	MnO	0.14	0.13	0.10	12.55	MnO	0.00	0.00	0.00
MgO	10.03	MgO	10.55	12.84	13.27	0.13	MgO	0.00	0.00	0.00
CaO	0.02	CaO	0.01	0.02	0.00	0.01	CaO	3.23	0.39	1.75
Na_2O	0.16	Na_2O	0.00	0.00	0.03	0.01	Na_2O	9.40	11.38	10.71
K_2O	8.69	K_2O	0.07	0.03	0.00	0.00	K_2O	0.35	0.05	0.08
Total	94.14	Total	87.77	87.27	88.05	88.49	Total	98.49	101.16	101.18
Si *apfu*	2.751	Si	2.670	2.657	2.700	2.620	Si	2.843	3.006	2.945
Al	1.727	Al	2.895	2.848	2.771	2.858	Al	1.159	0.005	1.050
Ti	0.105	Ti	0.007	0.008	0.006	0.008	Ti	0.000	0.000	0.000
Cr	0.002	Cr	0.000	0.004	0.001	0.003	Cr	0.000	0.000	0.000
Fe^{3+}		Fe^{3+}					Fe^{3+}			
Mg	1.134	Mg	1.684	2.034	2.081	1.976	Mg	0.000	0.000	0.000
Fe^{2+}	1.121	Fe^{2+}	2.600	2.342	2.337	2.462	Fe^{2+}	0.002	0.000	0.002
Mn	0.004	Mn	0.013	0.012	0.009	0.012	Mn	0.000	0.000	0.000
Ca	0.002	Ca	0.002	0.002	0.000	0.001	Ca	0.155	0.012	0.081
Na	0.024	Na	0.000	0.000	0.006	0.001	Na	0.816	0.951	0.899
K	0.841	K	0.010	0.004	0.001	0.000	K	0.020	0.003	0.004
Sum	7.712	Sum	9.881	9.911	9.912	9.941	Sum	4.995	4.977	4.981
X_{Mg}	0.503	X_{Mg}	0.393	0.465	0.471	0.445				

The structural formula of biotite is based on eleven atoms of oxygen. That of chlorite is based on fourteen atoms of oxygen, and that of plagioclase, on eight atoms of oxygen. $X_{Mg} = Mg/(Mg + Fe^{2+})$.

The zoned grains of garnet in mica schist E 514 show decreasing proportions of the grossular and spessartine components, and increasing proportions of the almandine and pyrope components, from core toward the rim. With the exception of the outermost rim, these trends are interpreted to have started growth at conditions of maximum pressure (Rötzler *et al.* 1998). For the high-pressure stage, a pressure estimate of about 12 kbar (phengite barometer of Massonne & Schreyer 1987, Massonne 1991) at temperatures of about 500–520°C (garnet–phengite thermometer of Green & Hellman 1982) has been deduced (Rötzler *et al.* 1998). Further growth occurred during decompression to about 8 kbar at increasing temperatures up to 600°C (TWEEQU method of Berman 1991). The lower-pressure stage of the P–T path was calculated on the basis of compositions of garnet near the rim (before the beginning of oscillatory zoning), plagioclase II, white mica II, biotite, ilmenite, rutile and quartz.

Oscillatory Zoning: Formation Due to Continuous Metamorphic Reactions Versus Formation Due to Fluid Control in an Open-System Environment

Indications of an open-system environment as a cause for the oscillatory zoning (*e.g.*, Jamtveit 1991, Yardley *et al.* 1991) were not found in the samples of this study. In only one other sample from locality E 514 (not treated here) was post-s_2 tourmaline found, which might be considered as evidence for late influx of fluid. Where oscillatory zoning is observed in the garnet grains of a sample, the number of oscillations and their relative changes in composition are the same in all grains throughout that sample. Moreover, although the localities of the mica schists E 514 and R 88 lie more than 15 km apart, the garnet grains of those samples still show the same number of major oscillations in Ca content. In contrast, garnet grains from an open-system

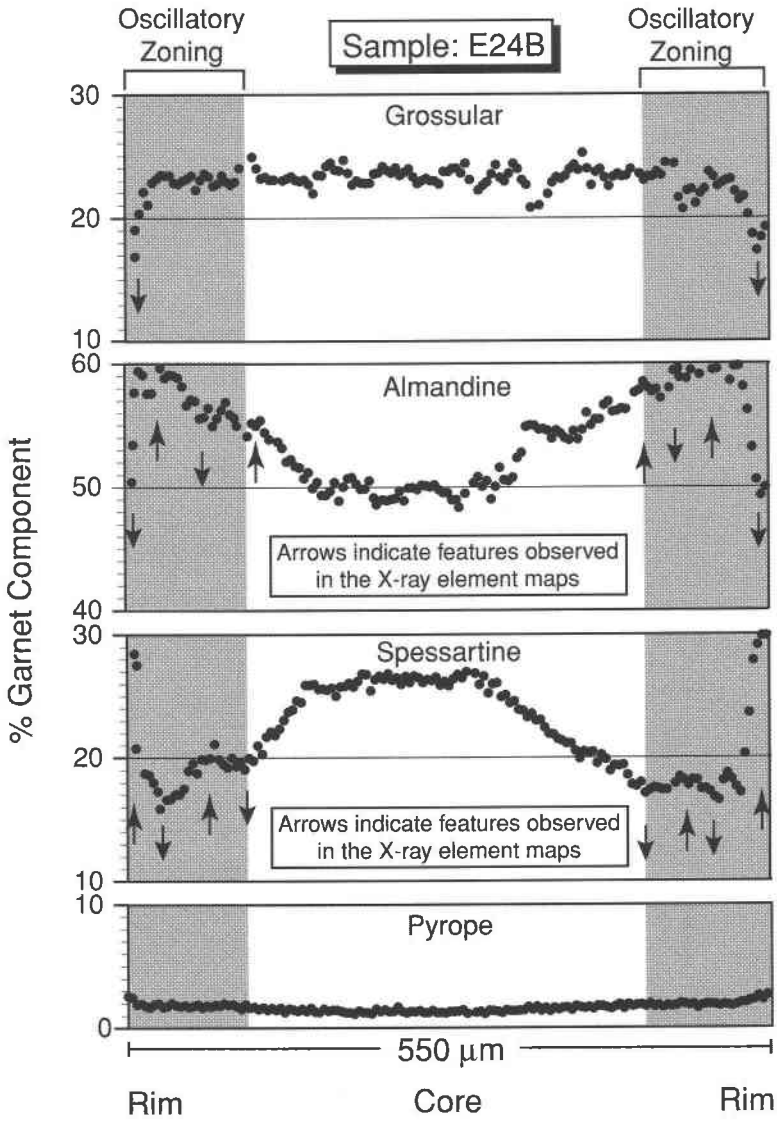

FIG. 9. Core–rim–core compositional profile of garnet from sample E 24B shown in Figure 3. Filled circles indicate locations of quantitative analyses. Gray shaded area indicates the outermost 100 μm edge of the grain where oscillatory zoning is observed.

environment tend to show highly variable and irregular patterns of oscillatory zoning, even within a single sample.

The high modal amounts and high Mn contents of the garnet and ilmenite from garnet phyllite E 24B, with up to 38 mole % spessartine component and up to 17 mole % pyrophanite component (7.64 wt % MnO), respectively, point to a Mn-rich bulk composition. This may explain the lack of oscillatory zoning in garnet grains from other samples of garnet phyllite poorer in Mn.

In Figures 13a and 13b, we present models illustrating how irregularities in the P–T path of uplift of the garnet phyllite and mica schist can lead to the observed oscillatory zoning in garnet. The P–T model in Figure 13a is based on the textures observed in thin section, the oscillations in Fe/Mn and the marked decrease of grossular component with respect to alman-

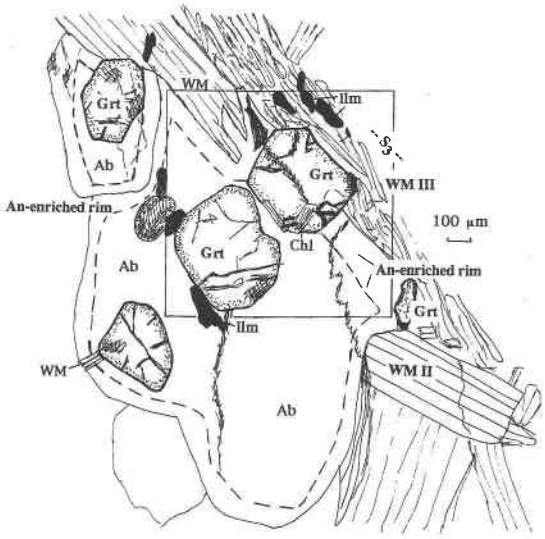

FIG. 10. Sketch of textural relationships in mica schist E 514. Two porphyroblasts of albite, each with an An-enriched rim, dominate this part of the thin section and enclose several subhedral grains of garnet. The Ca distribution for the two largest inclusions of garnet (area within the square) is shown in Figure 5. A typical MAPS analysis for Ca in the zoned albite porphyroblast is given in Figure 7. The upper-right garnet grain is only partially enclosed in albite. Note that the unprotected part has been corroded and sheared in s_3 shear zones.

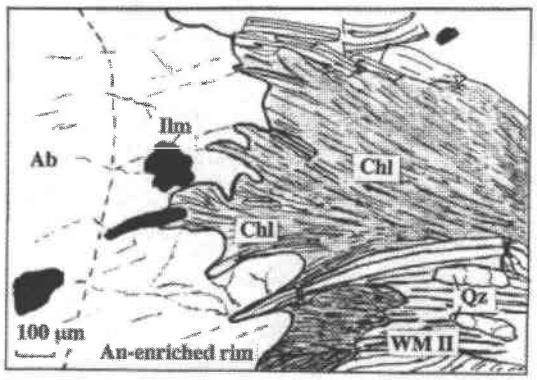

FIG. 11. Chlorite intergrown with An-enriched rim of albite porphyroblast from mica schist E 514.

dine + pyrope component toward the rim (Fig. 3c). Since clinozoisite is found as inclusions in the albite porphyroblasts, but is absent in the matrix, and chlorite is a common phase in the garnet phyllite, we postulate that both phases reacted to form garnet until one phase, clinozoisite, was consumed (Fig. 13a). This reaction is followed by a chlorite-consuming reaction that also consumed the An-component of the plagioclase. The liberated albite component formed the albite porphyroblasts, and the ratio of grossular to almandine + pyrope decreases sharply at the garnet rim owing to the change in the coefficients of the reaction products (Figs. 3c, 9). Even though there are no relics of oligoclase (Pl II) in this sample, it is likely that plagioclase richer in Ca was present before the albite porphyroblasts formed (*cf.* Rötzler 1995).

We propose that the zoning of the garnet is due to slight fluctuations in the decompression rate, causing a "wiggling" of the P–T path and concomitant changes in the phase equilibria responsible for garnet growth (Fig. 13a) (Schumacher *et al.* 1995). Slight overstepping of reactions led to disequilibrium in the Fe–Mn exchange reaction between garnet and ilmenite (see above).

In an analogous manner, the oscillatory changes in grossular and almandine concentrations of garnet from mica schist E 514 can be correlated with reactions involving garnet, chlorite and plagioclase (Fig. 13b). The textural criteria include relics of Al-enriched chlorite found as rare inclusions in garnet, and relics of plagioclase of oligoclase composition next to predominant albite porphyroblasts in the matrix. The oscillatory zones are found in both the matrix garnet (Fig. 4) as well as in garnet included in the albite porphyroblasts (Fig. 5). These observations suggest the following continuous garnet-producing reactions:

$$3\ \text{An} + 3\ \text{Chl} \rightarrow \text{Grs} + 5\ \text{Fe–Mg Grt} + 12\ H_2O \quad (1)$$

and

$$\text{Al-rich Chl} + \text{Qtz} \rightarrow \text{Fe–Mg Grt} + \text{Chl poorer in Al} + H_2O. \quad (2)$$

Reaction (1) leads to a garnet-core composition with a ratio of grossular to grossular + almandine + pyrope of 1 to 6 (Fig. 4). This value corresponds to garnet with 17 mole % grossular (Table 1). In contrast, reaction (2) does not produce any grossular component. Garnet growth due to an alternation of reactions (1) and (2) could produce the observations shown in Figure 4. Depending on the angle at which the "wiggling" P–T path crosses the P–T locations of the two reaction equilibria, a change in the relative proportion of the grossular component of the garnet with compositions between 0 to 16.7 mole % is possible. Compositions richer in grossular, as found in the core of garnet in Figure 5, could have been produced earlier during burial, when the P–T path crossed to the high-temperature side of reaction (1), but to the low-T side of reaction (2) (earliest part of the P–T path in Fig. 13b).

After the last local minimum in grossular component formed, the clockwise P–T path turned toward decreasing temperatures so that reaction (1) reversed

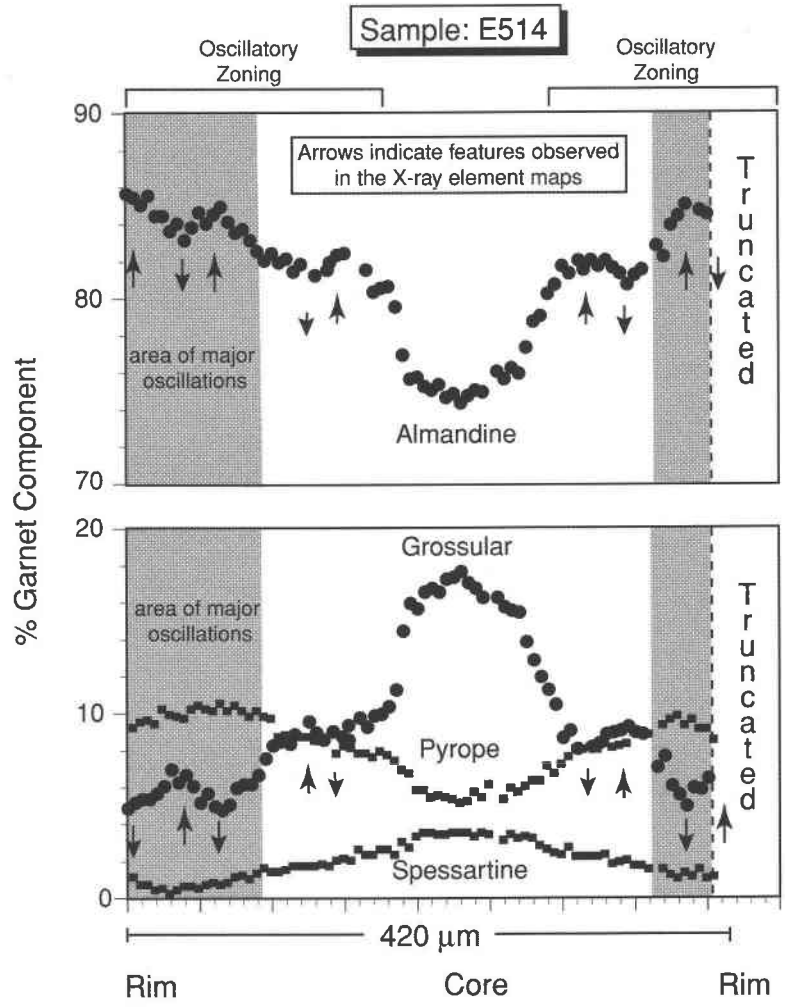

FIG. 12. Core–rim–core compositional profile of garnet that is shown in Figure 4. Filled circles and squares indicate location of quantitative analyses. Gray-shaded area indicates the outermost edge of the grain where major oscillatory zoning is observed.

(Fig. 13b). Chlorite and the An-enriched rim around the albite porphyroblasts formed, and garnet started to break down. Albite porphyroblasts rotated into s_3 shear zones exhibit an An-enriched rim with which the late chlorite is intergrown (Fig. 11). Garnet grains affected by the s_3 shear zones show clear signs of breakdown (Figs. 5, 10).

TEST FOR SUBSEQUENT MODIFICATION OF GARNET COMPOSITION DUE TO INTRACRYSTALLINE DIFFUSION

In order to validate the models outlined above, we considered the possibility of later modification of garnet composition due to intracrystalline diffusion, *i.e.*, a process that may have partially altered the pattern of zoning. The extent of possible intracrystalline modification of growth zonation is dependent on the maximum temperatures of metamorphism reached and the time required to reach the closure temperature, which can be deduced, to a first approximation, from the average rate of cooling. We assume here maximum temperatures of 600°C for mica schist E 514 and 500°C for garnet phyllite E 24. Average maximum rates of cooling of 20°C/Ma are assumed from available age data (see earlier).

Experimentally determined rates of diffusion for garnet differ considerably (see the summary by Schwandt *et al.* 1995), and reliable data for the intracrystalline rates of diffusion of Ca are completely

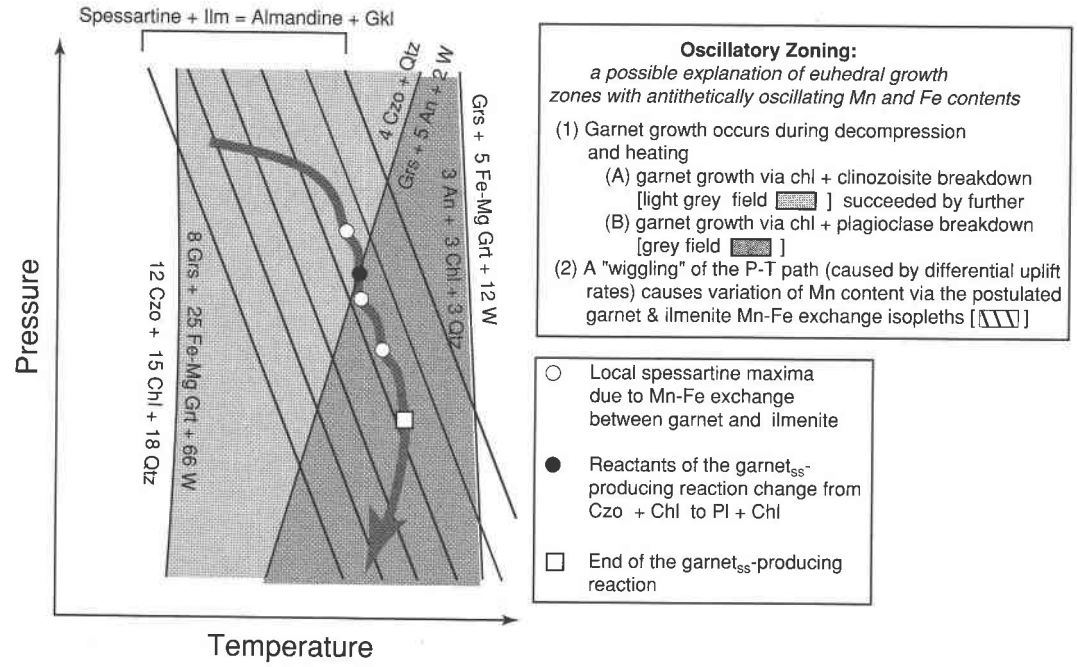

FIG. 13a. Schematic P–T diagram with phase equilibria that can explain the oscillatory zoning of garnet from garnet phyllite E 24B (see also legend). The slopes of the simplified reactions were calculated with the thermodynamic dataset of Berman (1988), as revised in 1992.

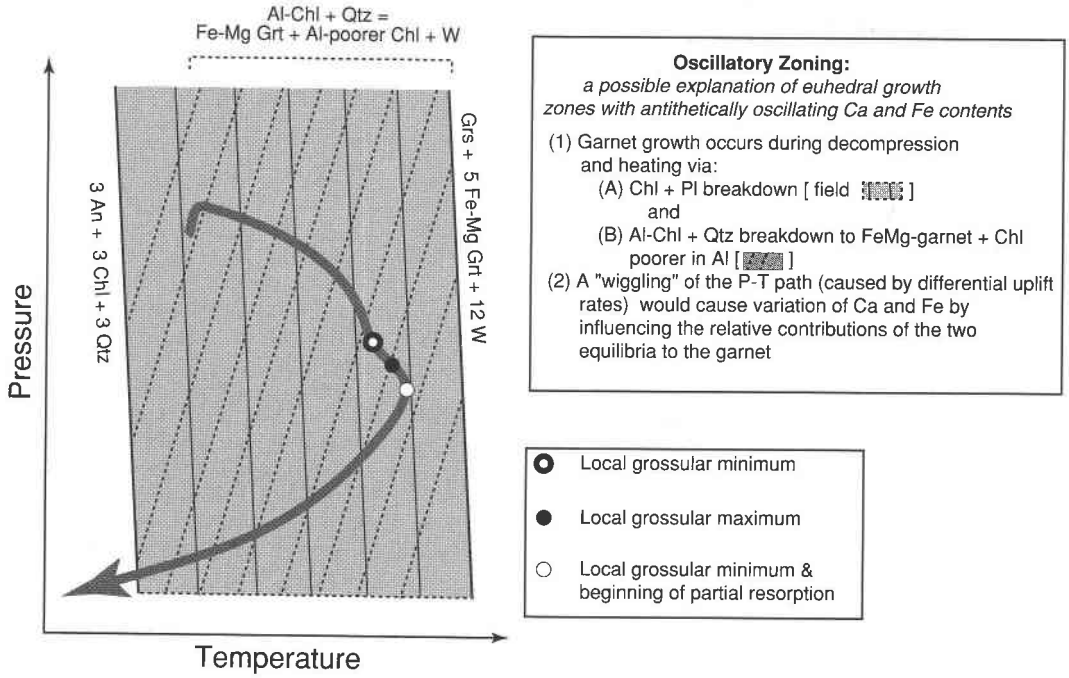

FIG. 13b. Schematic P–T diagram with phase equilibria that can explain the oscillatory zoning of garnet from mica schist E 514 (see also legend). The slopes of the simplified reactions were calculated with the thermodynamic dataset of Berman (1988), as revised in 1992.

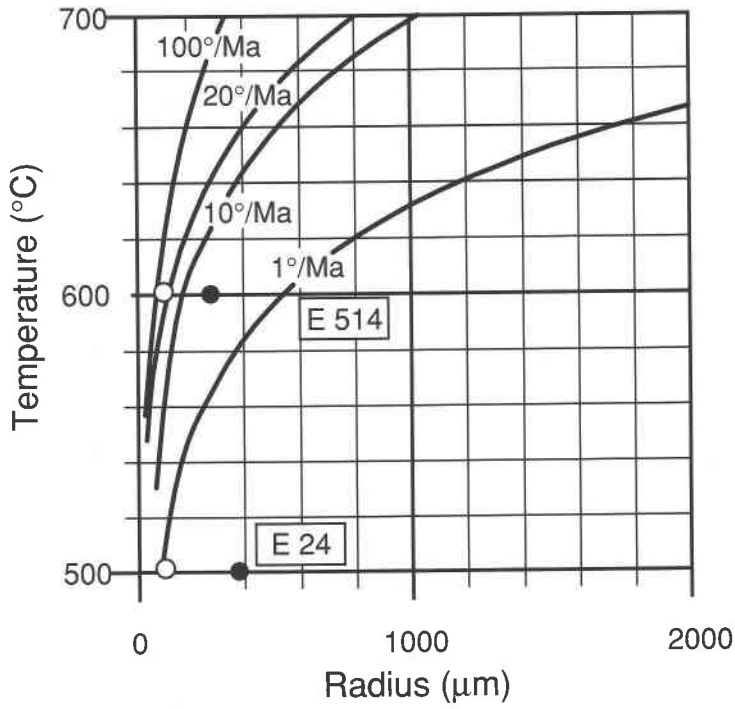

FIG. 14. Diagram after Dodson (1973) with garnet-closure temperature for Mg plotted against grain diameter (*i.e.*, length of diffusion path) for garnet grains from samples E 24B and E 514 (filled circles); open circles: diameter of the outer rim showing oscillatory zoning. The curves represent various rates of cooling, as indicated. Calculations based on data of Cygan & Lasaga (1985) for D_o, the diffusion coefficient at infinite T.

lacking. Nevertheless, all results in the recent literature indicate the relative rates of diffusion to be Ca < Mg < Fe < Mn. This means that the closure temperature for Mg may be reached while an exchange between Fe and Mn could still take place. In the following discussion, the data of Cygan & Lasaga (1985) and Schwandt *et al.* (1995) for Mg, and the data from Chakraborty & Ganguly (1991, 1992) for Fe, are applied to the garnet from garnet phyllite E 24B and mica schist E 514.

Figure 14 is based on the findings of Dodson (1973), with data from Cygan & Lasaga (1985), showing the relationship between the closure temperature T_c, the cooling rate and the diffusion of Mg for various grain-sizes [diagram based on D_o for Mg from Cygan & Lasaga (1985), with D_o being the diffusion coefficient at infinite T]. Because data on the "slower" Ca are not available, this plot can provide useful information on whether significant modification of antithetic Ca–Fe patterns of zoning could have occurred during cooling of the mica schists. Figure 14 suggests that this possibility cannot be ruled out for the outermost rim of the garnet from mica schist E 514. However, re-analysis of garnet from this sample with enhanced resolution showed additional minor oscillations nearer the core (Figs. 4, 12). This discovery further strengthens the argument that no post-growth homogenization has occurred. No modification of zoning involving Ca or Mg would be expected in garnet phyllite E 24B, so that the patterns of Ca and Mg zoning (Fig. 9) also clearly reflect growth zoning.

Figure 15a (after Spear 1991), based on diffusion data for Mg from Cygan & Lasaga (1985), shows the relationship between closure temperature, cooling rate and grain radius (*i.e.*, length of diffusion path) more clearly. For reference in the following discussion, we assume a critical diffusion-path of 100 μm (*cf.* Figs. 9, 12). Thus the intersection of the line labeled r = 0.01 cm in Figure 15 with a given cooling rate indicates, to a first approximation, the maximum temperature for which little or no modification of observed zoning profiles should be expected. Alternatively, given the temperature estimates of Rötzler *et al.* (1998) for the samples investigated here, a critical minimum rate of cooling can be estimated. Figure 15a indicates that mini-

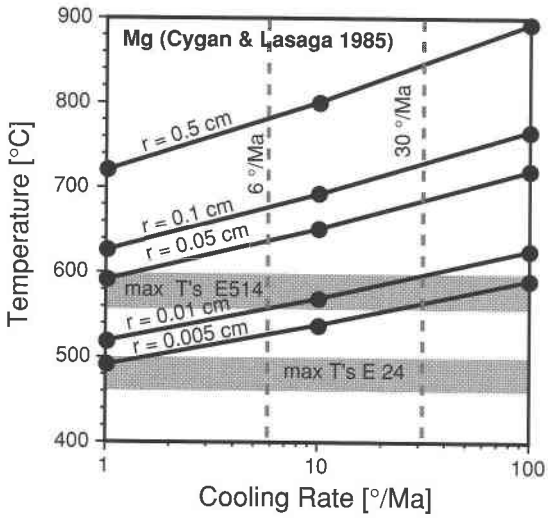

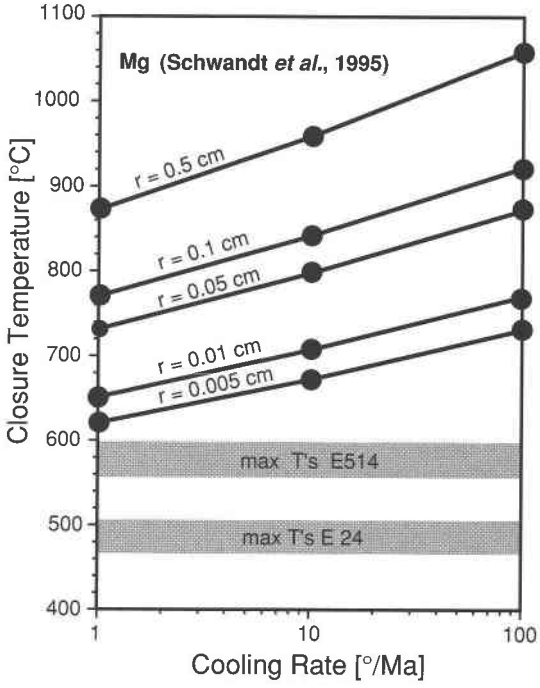

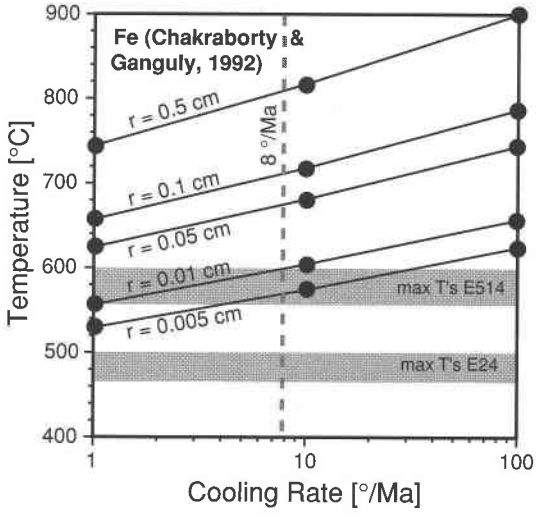

FIG. 15. Plots of closure temperature *versus* cooling rate for given radii (*i.e.,* length of diffusion path) of garnet grains (after Spear 1991). The temperature intervals shown in gray are estimates by Rötzler *et al.* (1998) of maximum temperatures reached by garnet phyllite E 24B and mica schist E 514. (a) Mg, diffusion data from Cygan & Lasaga (1985), (b) Mg, diffusion data from Schwandt *et al.* (1995), and (c) Fe, diffusion data from Chakraborty & Ganguly (1992).

mum rates of cooling of approximately 30°C/Ma would be required to avoid modification of a 0.01 cm zoning profile if cooling begins from peak temperatures of 600°C, the maximum temperatures of mica schist E 514 (*cf.* Rötzler *et al.* 1998). At slower rates of cooling, 1 to 6°C/Ma, and a radius r of the outermost garnet rim of 0.01 cm, these temperatures lie above the critical closure temperature. At cooling rates between 6 and 30°C/Ma, the temperature range intersects the line with the radius r = 0.01 cm. Considering the cooling rates discussed for the Western Erzgebirge, about 20°C/Ma, the closure temperature is 580°C. A later modification of the zoning pattern from the outermost rim of the garnet due to Fe–Mg or Fe–Mn exchange cannot be excluded. However, the diffusion of Ca is slower than Mg, and we therefore suggest that the observed antithetic zoning involving Ca–Fe is indeed a growth feature.

For the garnet phyllite, estimates of the peak metamorphic temperature of less than 520°C are assumed, and no modification should be expected, even at very low cooling rates of 1–2°C/Ma. If calculations are based on the Mg diffusion data of Schwandt *et al.* (1995) (Fig. 15b), who reported considerably slower diffusion for this cation, then our conclusion appears unequivocal for both the mica schists and the garnet phyllite. No intracrystalline diffusion could have modified the outermost 100-μm-wide rims.

Analogous calculations for the "faster" Fe, using diffusion data by Chakraborty & Ganguly (1991, 1992) are presented in Figure 15c. For the mica schists, diffusive homogenization appears possible if the cooling rate is less than 8°C/Ma. However, given our estimate of 20°C/Ma and the fact that the Fe zoning pattern clearly

correlates with the pattern of the much slower Ca, we suggest that the observed Fe profile also is a growth feature. As with Mg (and by inference, Ca also), the diffusion rate is too slow to achieve appreciable homogenization in garnet from garnet phyllite. Again, because of the clear correlation of Fe and Mn zoning patterns in these grains, we conclude that all observed concentration-profiles (Figs. 9, 12) are growth features.

Summary

Oscillatory patterns of zoning in regionally metamorphosed garnet may be more common than generally accepted, but can easily be missed during quantitative analysis or line traverses, because they may occur on the scale of a few μm. Sympathetic fluctuations in Fe, Mn and Ca are generally difficult to detect in electron back-scatter images because of the great similarity in average atomic number. The zoning patterns reported here did not show up in the electron back-scatter images, but were found by MAPS analysis.

To our knowledge, an interpretation of oscillatory zoning in regional metamorphic garnet has not yet been given in the literature. Bradshaw (1978) reported, but did not interpret, euhedral zones showing marginal enrichment in Mn, locally with euhedral Mn oscillations in garnet from type-C eclogite. Yardley *et al.* (1991) attributed various examples of oscillatory zoning in metamorphic minerals to growth under supersaturated conditions due to fluid infiltration. So far, no evidence in support of open-system behavior of the fluid phase could be found in the phyllites studied, and only locally in the mica schists could the zonation be interpreted as such (post-s_2 tourmaline around garnet in one out of three thin sections of sample E 514 could suggest influx of a B-bearing fluid). Consequently, and as demonstrated by the textural relationships, we attribute the oscillatory changes in garnet composition to regional metamorphic reactions that took place during garnet growth.

According to our model, the grains of garnet grew during a small to moderate T increase along the decompression part of the P–T path, with small variations in the rate of decompression, but without any noticeable infiltration of externally derived fluid (closed system). The irregular, fluctuating rates of exhumation would have caused a variation in the angle between the P–T path and the P–T slope of the continuous reaction equilibria involving garnet that it crossed. Therefore, at least two garnet-forming reactions contributed to the oscillating patterns of zoning of the garnet. The reaction curves could have been crossed metastably, leading to disequilibrium between the outermost rim and the matrix phases.

Considering a cooling rate of 20°C for the western Erzgebirge, and available data for cation diffusion in garnet, we can conclude that modification of the observed patterns of zoning in garnet during cooling and decompression is unlikely.

Acknowledgements

We thank John C. Schumacher (Bristol) for constructive discussions and support with graphical presentation. R.J. Tracy and T. Menard provided critical and in part adrenalin-generating comments that much improved our presentation. The X-ray distribution maps shown in Figures 3 and 4 improved greatly through re-analysis by Heinz-Jürgen Bernhardt (Bochum); his contribution is much appreciated. We thank Editor R.F. Martin and guest Associate Editor D.R.M. Pattison for their advice and support. This work was supported by grants of the Deutsche Forschungsgemeinschaft (Ma 689/6–1, Ma 689/6–2 and Ma 689/11), which are gratefully acknowledged.

References

Berman, R.(1988): Internally-consistent thermodynamic data for minerals in the system Na_2O–K_2O–CaO–MgO–FeO–Fe_2O3–Al_2O_3–SiO_2–TiO_2–H_2O–CO_2. *J. Petrol.* **29**, 443-522.

_____ (1991): Thermobarometry using multi-equilibrium calculations: a new technique, with petrological applications. *Can. Mineral* **29**, 833-855.

Bradshaw, J.Y. (1978): *Petrology and Mineralogy of Interlayered Eclogite and High-Grade Blueschist from the Franciscan Formation, California.* M.Sc. thesis, Univ. of Calgary, Calgary, Alberta.

Chakraborty, S. & Ganguly, J. (1991): Compositional zoning and cation diffusion in garnets. *In* Diffusion, Atomic Ordering, and Mass Transport (J. Ganguly, ed.). Springer, New York, N.Y. (121-175).

_____ & _____ (1992): Cation diffusion in aluminosilicate garnets: experimental determination in spessartine–almandine diffusion couples, evaluation of effective binary diffusion coefficients, and applications. *Contrib. Mineral. Petrol.* **111**, 74-86.

Cygan, R.T. & Lasaga, A.C. (1985): Self diffusion of magnesium in garnet at 750° to 900°C. *Am. J. Sci.* **285**, 328-350.

Dodson, M.H. (1973): Closure temperature in cooling geochronological and petrological systems. *Contrib. Mineral. Petrol.* **40**, 259-274.

Evans, B.W. & Guidotti, C.V. (1966): The sillimanite – potash feldspar isograd in W. Maine, USA. *Contrib. Mineral. Petrol.* **12**, 25-62.

Ganguly, J. & Saxena, S.K. (1984): Mixing properties of aluminosilicate garnets: constraints from natural and experimental data, and applications to geothermobarometry. *Am. Mineral.* **69**, 88-97.

GERSTENBERGER, H. (1989): Autometasomatic Rb enrichments in highly evolved granites causing lowered Rb–Sr isochron intercepts. *Earth Planet. Sci. Lett.* **93**, 65-75.

GREEN, T. H. & HELLMAN, P.L. (1982): Fe–Mg partitioning between coexisting garnet and phengite at high pressure, and comments on a garnet–phengite geothermometer. *Lithos* **15**, 253-266.

JAMTVEIT, B. (1991): Oscillatory zonation patterns in hydrothermal grossular–andradite garnet: nonlinear dynamics in regions of immiscibility. *Am. Mineral.* **76**, 1319-1327.

_____ & ANDERSEN, T.B. (1992): Morphological instabilities during rapid growth of metamorphic garnets. *Phys. Chem. Minerals* **19**, 176-184.

_____, WOGELIUS, R.A. & FRASER, D.G. (1993): Zonation patterns of skarn garnets: records of hydrothermal system evolution. *Geology* **21**, 113-116.

KOSSMAT, F. (1925): *Übersicht über die Geologie von Sachsen.* Dt. Verlag Leipzig, 1-129.

KOTKOVÁ, J., KRÖNER, A., TODT, W. & FIALA, J. (1996): Zircon dating of North Bohemian granulites, Czech Republic: further evidence for the Lower Carboniferous high-pressure event in the Bohemian Massif. *Geol. Rundschau* **85**, 154-161.

KRENTZ, O. (1984): Temperaturregime und Altersstellung der regionalen Metamorphose im mittleren Erzgebirge. *Freiberger Forschungshefte* **C 390**, 212-228.

KRETZ, R. (1983): Symbols for rock-forming minerals. *Am. Mineral.* **68**, 277-279.

KROHE, A. (1996): Variscan tectonics of central Europe: postaccretionary intraplate deformation of weak continental lithosphere. *Tectonics* **15**, 1364-1388.

KRÖNER, A. & WILLNER, A. (1995): Magmatische und metamorphe Zirkonalter der Gneis-Eklogit-Einheit des Erzgebirges. *Terra Nostra* **8**, 112 (abstr.).

LORENZ, W. & HOTH, K. (1964): Die lithostratigraphische Gliederung des kristallinen Vorsilurs der Fichtelgebirgisch-Erzgebirgischen Antiklinale. *Geologie* **13**, *Beiheft* **44**, 1-44.

_____ & _____ (1990): Lithostratigraphie im Erzgebirge – Konzeption, Entwicklung, Probleme und Perspektive. *Abhandlungen des Staatlichen Museum für Mineralogie und Geologie zu Dresden* **37**, 7-35.

MASSONNE, H.J. (1991): *High-Pressure, Low-Temperature Metamorphism of Pelitic and Other Protholiths Based on Experiments in the System K_2O–MgO–Al_2O_3–SiO_2–H_2O.* Habilitation thesis, Ruhr-Universität Bochum, Bochum, Germany.

_____ (1992): Thermochemical determination of water activities relevant to eclogitic rocks. *In* Proc. 7th Int. Symp. on Water–Rock Interaction (Y.K. Kharaka & A.S. Maest, eds.). Balkema, Rotterdam, The Netherlands (A29-A32).

_____ (1994): P–T evolution of eclogitic lenses in the crystalline complex of the Erzgebirge, Middle Europe: an example for high-pressure to ultrahigh-pressure metabasites incorporated into continental crust. *Workshop on ultrahigh-pressure metamorphism and tectonics (Stanford)* **1**, A29-A32 (extended abstr.).

_____ & SCHREYER, W. (1987): Phengite geobarometry based of the limiting assemblage with K-feldspar, phlogopite and quartz. *Contrib. Mineral. Petrol.* **96**, 212-224.

POWNCEBY, M.I., WALL, V.J. & O'NEILL, H.ST.C. (1987): Fe–Mn partitioning between garnet and ilmenite: experimental calibration and applications. *Contrib. Mineral. Petrol.* **97**, 116-126.

ROBINSON, P. (1991): The eye of the petrographer, the mind of the petrologist. *Am. Mineral.* **76**, 1781-1810.

RÖTZLER, K. (1995): Die P–T-Entwicklung der Metamorphite des Mittel- und Westerzgebirges. *GeoForschungsZentrum Potsdam, Sci. Tech. Rep.* **STR96/4**.

_____ (1997): Formation of barian phengites in eclogites from the Erzgebirge, Germany. *Berichte der Deutschen Mineralogischen Gesellschaft, Beih. Z., Eur. J. Mineral.* **9**(1).

_____, SCHUMACHER, R., MARESCH, W.V. & WILLNER, A.P. (1998): Characterization and geodynamic implications of contrasting metamorphic evolution in juxtaposed high-pressure units of the western Erzgebirge, Saxony, Germany. *Eur. J. Mineral.* **10**, 261-280.

SCHMÄDICKE, E., METZGER, K. COSCA, M.A. & OKRUSCH, M. (1995): Variscan Sm–Nd and Ar–Ar ages of eclogite facies rocks from the Erzgebirge, Bohemian Massif. *J. Metamorphic Geol.* **13**, 537- 552.

_____, OKRUSCH, M. & SCHMIDT, W. (1992): Eclogite-facies rocks in the Saxonian Erzgebirge, Germany: high pressure metamorphism under contrasting P–T conditions. *Contrib. Mineral. Petrol.* **110**, 226-241.

SCHUMACHER, R., RÖTZLER, K. & MARESCH, W.V. (1995): Oscillatory zoning in regional metamorphic garnets from the Westerzgebirge and their tectonic framework. *EUG 8 (Strasbourg), Abstr. suppl.* **1** to *Terra nova* **7**, 311.

SCHWANDT, C.S., CYGAN, R.T. & WESTRICH, H.R. (1995): Mg self-diffusion in pyrope garnet. *Am. Mineral.* **80**, 483-490.

SPEAR, F.S. (1991): On the interpretation of peak metamorphic temperatures in light of garnet diffusion during cooling. *J. Metamorphic Geol.* **9**, 379-388.

WILLNER, A.P., KRÖNER, A. & TEUFEL, S. (1996): Time of formation, peak of HP-metamorphism and cooling history of quartz-feldspar rocks from the central Erzgebirge (Saxony/Germany). *International Goldschmidt Conference (Heidelberg), Abstr.* **1**, 675.

_____, RÖTZLER, K., KROHE, A., MARESCH, W.V. & SCHUMACHER, R. (1994): Druck–Temperatur–Deforma-

tions-Entwicklung verschiedener Krusteneinheiten im Erzgebirge. Eine Modellregion für die Exhumierung von Hochdruck-Gesteinen. *Terra Nostra* **94**, 104-106.

_____, _____ & MARESCH, W.V. (1997): Pressure–temperature and fluid evolution of quartzofeldspathic metamorphic rocks with a relic high-pressure, granulite-facies history from the central Erzgebirge (Saxony, Germany). *J. Petrol.* **38**, 307-336.

YARDLEY, B.W.D., ROCHELLE, C.A., BARNICOAT, A.C. & LLOYD, G.E. (1991): Oscillatory zoning in metamorphic minerals: an indicator of infiltration metasomatism. *Mineral. Mag.* **55**, 357-365.

Received April 1, 1998, revised manuscript accepted February 10, 1999.